Received: 16 June 2021 | Accepted: 22 November 2021

DOI: 10.1111/liv.15115

Liver INTERNATIONAL WILEY

ORIGINAL ARTICLE

Molecular mechanism of albumin in suppressing invasion and metastasis of hepatocellular carcinoma

Xiao Fu | Yixuan Yang | Dazhi Zhang

Department of Infectious Diseases, Key Laboratory of Molecular Biology for Infectious Diseases, Institute for Viral Hepatitis, the Second Affiliated Hospital of Chongqing Medical University, Chongqing, People's Republic of China

Correspondence
Dazhi Zhang, Department of Infectious Diseases, Key Laboratory of Molecular Biology for Infectious Diseases, Institute for Viral Hepatitis, the Second Affiliated Hospital of Chongqing Medical University, Chongqing 400010, People's Republic of China.
Email: 300595@hospital.cqmu.edu.cn

Funding information
This study was supported by the Chinese National 13th Five-Year Plan's Science and Technology Projects (2017ZX10203202-001/2017ZX10203202-002).

Handling Editor: Alejandro Forner

Abstract

Background & Aims: Worldwide, hepatocellular carcinoma (HCC) is one of the most common causes of death in people. Albumin (ALB) is considered as an important indicator for HCC prognosis, and evidence has shown HCC cell growth can be regulated by ALB. However, the role of ALB in hepatocarcinogenesis and the mechanism of action is still unknown.

Methods: The expression of ALB was determined by clinical profiles, immunohistochemistry, and western blot. Wound healing and Transwell assays were conducted to evaluate the effects of ALB during migration and invasion in HCC. We used mass spectrometry coupled isobaric tags for relative and absolute quantitation (iTRAQ)-technology to identify secretory differentially expressed proteins (DEPs) in ALB knockdown HepG2 cells. Western blot, reverse transcription-quantitative polymerase chain reaction and enzyme-linked immunosorbent assay techniques were used for verification.

Results: We suggested that ALB was associated with aggressive metastasis and depleting ALB significantly promoted invasion and migration of HCC. A total of 210 DEPs were identified after silencing of ALB. We observed that a negative correlation between ALB and urokinase plasminogen activator surface receptor (uPAR) expression levels.

Conclusions: ALB acts as a tumour suppressor and plays a key role in HCC progression, particularly in invasion and metastasis. Suppression of ALB promoted migration and invasion of HCC cells by increasing uPAR, matrix metalloproteinase (MMP2), and MMP9.

KEYWORDS
albumin, hepatocellular carcinoma, isotope tags for relative and absolute quantitation, urokinase plasminogen activator surface receptor

Abbreviations: AFP, α-fetoprotein; ALB, albumin; ALF, alpha-albumin; AZGP1, zinc alpha2 glycoprotein; BCA, bicinchoninic acid assay; BMP2, bone morphogenetic protein 2; CHB, chronic hepatitis B; CRP, C-reactive protein; CTSD, cathepsin D; CTSF, Cathepsin F; DEPs, differentially expressed proteins; ELISA, enzyme-linked immunosorbent assay; EMT, epithelial–mesenchymal transition; FBS, fetal bovine serum; GPC3, glypican-3; HCC, hepatocellular carcinoma; IDH2, isocitrate dehydrogenase 2; iTRAQ, isobaric tags for relative and absolute quantitation; LC, liver cirrhosis; LCN2, lipocalin 2; MMPs, matrix metalloproteinases; MS, mass spectrometry; MTD, maximum tumour diameter; NOTCH1, neurogenic locus notch homolog protein 1; PVT, portal vein thrombosis; RPS3A, ribosomal protein S3a; RT-qPCR, reverse transcription-quantitative polymerase chain reaction; SI, staining index; uPAR, urokinase plasminogen activator surface receptor.

1 | INTRODUCTION

Hepatocellular carcinoma (HCC) ranks sixth in malignant tumour detection and fourth in cancer-induced death.[1] Despite the significant progress has been made in HCC diagnosis and treatment, HCC retains a poor prognosis, and the 5-year survival rate remains approximately 18%.[2,3] HCC prognosis is related to tumour size, α-fetoprotein (AFP), nodules, portal vein thrombosis (PVT), the extent of vascular invasion and TNM stage.[4-6] More recently, inflammation-based markers have been used to determine prognosis for several tumour types, including HCC. The Glasgow Score and C-reactive protein (CRP) to albumin ratio are important indicators.[7,8] Although AFP and CRP have been studied, the relationship between ALB and HCC remains unclear.

There are four genes encoding albumin (ALB), alpha-albumin (ALF), alpha-fetoprotein (AFP) and vitamin D-binding protein. ALB is the most abundant protein in extracellular fluids and is exclusively synthesized by hepatocytes and released into the circulation at a rate of about 13–14 g per day.[9] It has been reported that lower albumin levels are associated with larger HCC tumors.[10] However, previous studies suggested that increased albumin levels can inhibit HCC growth.[11,12] Although ALB is considered as an indicator and has been investigated in various cancers, its effect is still unclear on the metastasis of liver cancer.

The application of isobaric tags for relative and absolute quantitation (iTRAQ) method is widely accepted for identification of differentially expressed protein (DEP) and protein interactions.[13] With the ability to analyse eight samples simultaneously, this method effectively reduces the potential mistakes during repeated sample testing.[14] In the present study, we found evidence that ALB is related to the metastasis of HCC through clinical investigation and immunohistochemistry. We investigated the effect ALB exerts on liver cancer cells (HepG2 and Huh7). To illustrate the potential molecular mechanism, iTRAQ-based mass spectrometry (MS) technology was applied to analyse secretory DEPs in HepG2 cells either with or without a silenced ALB gene.

Lay summary

This study provides a novel way for further examination of mechanism of ALB in HCC and rises the possibility of therapeutically targeting ALB for the treatment liver cancers.

2 | MATERIALS AND METHODS

2.1 | Reagents and antibodies

The L02, Hep3B, Huh7, HepG2, and MHCC97H cell lines was accessed from the Chinese Academy of Sciences (Shanghai, China). The iTRAQ eight-plex kits were purchased from Applied Biosystems (Thermo Fisher Scientific, Inc., Waltham, MA, USA). The Transwell kit was ordered from Cell Biolabs (San Diego, CA, USA). The electrophoresis reagents related to western blotting were from by Bio-Rad Laboratories (Hercules, CA, USA) and the polyvinylidene fluoride (PVDF) membranes were manufactured by GE Healthcare (Chicago, IL, USA). Antibodies against AZGP1 (ab180574), GPC3 (ab174851), NOTCH1 (ab52627), CTSD (ab75811), BMP2 (ab14933), LCN2 (ab125075), RPS3A (ab171742), urokinase plasminogen activator surface receptor (uPAR) (ab103791), MMP2 (ab181286) and MMP9 (ab137867) were from Abcam (Cambridge, MA, USA). Albumin (4929) was from Cell Signaling Technology, Inc. (Danvers, MA, USA). IDH2 (DF8561), E-cadherin(AF0131), N-cadherin(AF4039), vimentin(AF0292), Snail(AF6032), Twist(AF4009) and β-actin (AF7018) were obtained from Affinity Biosciences (Cincinnati, OH, USA); Albumin (HSS100359) (HSS100358) (HSS176651)-specific siRNAs and negative control siRNA (12935-400) and the forward/reverse primers used in reverse transcription-quantitative polymerase chain reaction (RT-qPCR) were ordered from Invitrogen (Thermo Fisher Scientific, Inc.) RPS3A (Gene ID: 6189), NOTCH1 (Gene ID: 4851) and uPAR (Gene ID: 5329)-specific siRNAs were designed by Gene-Pharma (Suzhou, China).

2.2 | Patients and specimens

We analysed, retrospectively, 632 patients with HCC treated at the Second Affiliated Hospital of Chongqing Medical University in Chongqing between December 2014 and 2019, who had complete baseline tumour data, including tumour size, tumour nodules number, PVT and plasma AFP levels, full blood counts, and tests of albumin, AST and total bilirubin. A total of 50 human liver tissues were obtained through partial liver resection of HBV-related patients with HCC in our hospital from September 2020 to February 2021. None of the patients were treated with any adjuvant therapy before surgery and were identified by two pathologists. Table 3 details the patients' clinical characteristics. For the validation phase, 108 serum specimens were obtained from patients with chronic hepatitis B (CHB, n = 19), liver cirrhosis (LC, n = 19), HCC (HCC and ALB ≥3.5 g/dL, n = 36 and HCC and ALB < 3.5 g/dL, n = 34). All enrolled patients met the criteria of HCC diagnosis as defined by the American Association for the Study of Liver Diseases.[15] Signed, informed consent forms were collected from each patient prior to their inclusion in our study, and the study was approved by the Ethics Committee of Chongqing Medical University.

2.3 | Immunohistochemistry

Liver tissue samples were deparaffinized with xylene, rehydrated with an ethanol gradient and washed with double-distilled H_2O. Tissues were soaked in 3% H_2O_2 for 10 minutes to remove endogenous peroxidase. The tissue samples were blocked with BSA for 30 minutes and incubated with ALB primary antibodies at 4°C

overnight. A DAKO EnVision+System, HRP (DakoCytomation, Glostrup, Denmark) was used to detect the expression of ALB under 200× magnification. Intensity of nuclear staining was graded as 0 (negative), 1 (weak), 2 (moderate) or 3 (strong). The number of positive cells received a score of 0 (0%), 1 (1%-25%), 2 (26%-50%), 3 (51%-75%) or 4 (76%-100%). The staining index (SI) was taken by multiplying the nuclear staining score by the positive cell score to obtain a total score of 0-12. The cut-off value was set to 6 (median SI value). In this study, a total score of 6 or less was defined as low expression, and more than 6 was defined as high expression.

2.4 | Cell culture and transfection

The L02, Hep3B, Huh7, HepG2 and MHCC97H cell lines were maintained in high glucose DMEM (KeyGen Biotech, Nanjing, China) with 10% fetal bovine serum (FBS) (Excell Bio, Shanghai, China) at 37°C with 5% CO_2 and 95% relative humidity. Huh-7 and HepG2 cells were transfected with 150 nM ALB-specific siRNA, RPS3A-specific siRNA, NOTCH1-specific siRNA, uPAR-specific siRNA or a negative control siRNA in a mixture of Lipofectamine® 2000 (Thermo Fisher Scientific) and Opti-MEM (Thermo Fisher Scientific, Inc.). The transfected cells were cultured in high glucose DMEM without penicillin or streptomycin antibiotics plus 10% FBS. RNA and protein were extracted at 24 and 48 hours.

2.5 | Wound healing and Transwell assays

Huh-7 and HepG2 cells were transfected with ALB-siRNA and negative control siRNA for the wound healing and Transwell assays. Cells were plated in 6-well plates and grown for 48 hours. A scratch was created in the cell monolayer using a 200-μL pipette tip, using a ruler as a guide. Cellular debris was removed by washing with PBS. Cell migration was identified by observing closure of the wound from 0 to 24 hours under 10× magnification. In the Transwell assays, an equal number of transfected cells (2×10^4 cells) were cultured in the upper chamber with 0.2 mL serum-free media, and 0.6 mL (DMEM plus 20% FBS was placed in the lower chamber. After 48 hours, the cells were fixed with methanol and stained with crystal violet. Cotton swabs were used to remove cells from the upper chamber. Invading cells in the bottom chamber were counted by microscopy using five random fields. Western blot analysis was performed to determine ALB downregulation. All experiments were performed in triplicate.

2.6 | Protein collection and ITRAQ labelling

After 48 hours of transfection, the supernatant was replaced with high glucose DMEM (KeyGen Biotech) without penicillin and the cells incubated for another 2 days. The supernatants were collected and filtered using a 0.22-μm filter (Millipore, Bedford, MA, USA). Secretory proteins were concentrated using an Amicon® centrifugal filter (Billerica, MA, USA). Bicinchoninic acid assay (BCA) was used to determine protein concentration. After resuspending proteins in dissolution buffer, denaturing and cysteine blocking, the proteins were digested with trypsin based on the iTRAQ standard protocol. Protein samples with negative control siRNA were labelled 114, 115 and 116, and the proteins treated with ALB knockdown siRNA were labelled 117, 118 and 119. The labelled samples were combined before analysis.

2.7 | Peptide fractionation

The labelled peptide samples were resolubilized in 1% Pharmalyte (Sigma-Aldrich, St. Louis, MO, USA) and 8 M urea. The processed samples were electrotransferred to rehydrated IPG strips (pH 3–10, GE Healthcare, UK) for 14 hours at 30 V.[16] Peptides were focused successively for 68 kV·h on an IPG phor (GE Healthcare). The strips were cut into pieces. Peptide extraction was performed by incubating the gel pieces in 100 μL buffer including 2% acetonitrile and 0.1% formic acid. The fractions were lyophilized and purified on a C-18 Discovery® DSC-18 SPE column (100 mg capacity, Sigma-Aldrich), and stored at −20°C for LC-MS/MS analysis.

2.8 | Mass spectrometry

MS analysis was carried out on a QStar Elite mass spectrometer (Applied Biosystems, Foster City, CA, USA) coupled with an online Dionex UltiMate 3000 system (Thermo Fisher Scientific, Amsterdam, The Netherlands).[16,17] Lyophilized samples were resuspended in buffer A and loaded onto a C18 trap column for peptide separation. Samples were eluted at 300 nL/min in a gradient from 2% to 100% mobile phase B (98% acetonitrile and 0.1% formic acid). A mass range of 300–1800 *m/z* was selected for data acquisition in the positive ion mode. The two most intensely charged peptides above 20 counts with a dynamic exclusion of 30 seconds ± 50 mDa were selected. ProteinPilot v2.0 (Applied Biosystems, Waltham, MA, USA) was applied for protein identification and quantification. The UniProt database (http://www.uniprot.org/) was used to identify proteins from the MS/MS analysis. For the identified proteins, we considered a fold-change >2(2/1) or <0.5 (1/2), and each protein contained at least two peptides as a trusted protein.

2.9 | Bioinformatics analysis

All identified proteins were assessed by a Gene Ontology analysis. The distribution of cellular components, biological processes and molecular functions were conducted via PANTHER (http://www.pantherdb.org/).

2.10 | Reverse transcription-quantitative polymerase chain reaction

The cell pellet was lysed, centrifuged and extracted RNA. According to the RNA concentration, 2 μL of reverse transcriptase, nuclease-free water and 5× RT Mix were added for a total cDNA reverse transcription reaction volume of 20 μL. For the 20 μL reaction, we added 10 μL TB green, 0.8 μL forward primer, 0.8 μL reverse primer, 2 μL DNA and 6.4 μL nuclease-free water in each tube. A Fast PCR kit (KAPA Biosystems, Wilmington, MA, USA) was applied for RT-qPCR with primers for LCN2 (NM_005564), CTSD (NM_001909), GPC3 (NM_004484), NOTCH1 (NM_017617), RPS3A (NM_001006), CTSF (NM_003793), BMP2 (NM_001200), GAPDH (NM_002046), AZGP1 (NM_001185) and PLAUR (NM_002659). The results were analysed using the $2^{-\Delta\Delta Cq}$ method,[18] where the expression of the control group was considered as 1, such that error bars were not available for the control group.

2.11 | Western blot

Forty eight hours transfected cells were collected and lysed. The cell suspension was pelleted by centrifugation at 12 000 rpm for 4 minutes and the intracellular protein was collected. Additionally, the secretory proteins were ultrafiltered with Amicon® Ultra-15 centrifugal filter devices at 5000 *g* for 30 minutes, and extracellular protein was obtained. Protein concentration was measured using a BCA kit. 60 μg of protein was separated via 10% SDS-PAGE and the proteins were transferred to PVDF membranes. The blots were blocked for 1h at RT with 5% BSA or 5% skimmed powdered milk in TBST. The blots were incubated with primary antibodies overnight at 4°C, and washed with TBST and incubated for 1h at RT with HRP-IgG antibodies. The blots were washed again with TBST. ECL reagents were prepared at a ratio of 1:1, and the bands were analysed using a ChemiDoc MP imaging system (Bio-Rad Laboratories).

2.12 | Gelatin zymography

First, we use an ultrafiltration centrifuge tube to concentrate the culture supernatant five times, and the supernatant was frozen at −80° for later use. The samples were mixed with an equal volume of 2× non-reducing buffer (4% SDS, 100 mmol l^{-1} Tris-Cl, 20% glycerol, 0.02% bromophenol blue) and 15–20 μL was loaded per well. Samples were electrophoresed on 8% SDS polyacrylamide gels containing 1 mg/mL gelatin. Then, the gels were washed twice for 15 minutes in 2.5% Triton X-100 to remove SDS and incubated overnight at 37°C in substrate buffer (50 mmol l^{-1} Tris-HCl, pH 7.5, 5 mmol l^{-1} $CaCl_2$ and 0.02% NaCl). The gels were stained with Coomassie Brilliant Blue for 1 hour and destained in washing solution (30% methanol, 10% acetic acid). The gelatinolytic activity was determined as horizontal white bands on a blue background.

2.13 | Enzyme-linked immunosorbent assay

Levels of serum uPAR were measured in all 108 validation cohort samples using commercially available human uPAR enzyme-linked immunosorbent assay (ELISA) kits (#ELH-uPAR, Raybiotech, Peachtree Corners, GA, USA), according to the standard protocol. The samples were thawed on ice, and all reagents were equilibrated to room temperature.

2.14 | Statistical analysis

Each experiment was conducted at least in triplicate. The data were presented as the mean ± standard deviation (SD). Statistical analysis was performed using SPSS 26.0 (IBM Corp., Armonk, NY, USA) for the Student's *t*-test for clinical analysis. The chi-square and the Mann–Whitney test were applied for qualitative variables. Spearman's correlation was used to determine the association between two continuous variables because the distributions were nonnormal. The data graphing was performed using GraphPad Prism (version 8.3). The *P* value of less .05 was statistically significant.

3 | RESULTS

3.1 | Correlation between albumin and clinicopathological features of patients with HCC

According on the serum levels of albumin, HCC samples were grouped into one group with more than 3.5 g/dL and another one with less than 3.5 g/dL. Tumour parameters such as tumour nodule, PVT, maximum tumour diameter (MTD) and AFP between the two groups were compared. The data indicated that the low albumin expression levels were significantly correlated with aggressive tumours (such as higher MTD; $P < .001$, chi-squared test), number of tumour nodules ($P < .001$, chi-squared test), presence of PVT ($P < .001$, chi-squared test) and blood AFP levels of the patients (Table 1). This analysis was conducted again in patients with bilirubin levels <2.0 mg/mL, and a consistent dissimilarity was observed between patients with normal and patients with low serum albumin levels (Table 2).

3.2 | Albumin expression is downregulated in HCC tissues

A total of 50 patients had gene expression data for both paracancerous and tumour samples. The expression of ALB between the HCC paracancerous samples and the tumour samples of the same patient were compared. Strong staining of ALB was observed in the paracancerous samples (Figure 1A). Albumin expression was significantly downregulated in HCC samples compared with paracancerous samples ($P < .05$) (Figure 1B). The correlation between

TABLE 1 Comparisons between HCC patients with serum albumin dichotomized into <3.5 or ≥3.5 g/dL

	Small tumours (<5 cm diameter)			Large tumours (≥5cm diameter)		
	Albumin <3.5	Albumin ≥3.5		Albumin<3.5	Albumin≥3.5	
	(n = 115)	(n = 121)	*P* value[a]	(n = 272)	(n = 124)	*P* value[a]
Parameter	(a)	(b)	(a) vs (b)	(c)	(d)	(c) vs (d)
Platelet count (×10^9/L)	110.03 ± 90.36	113.84 ± 69.09	.144	159.89 ± 93.36	163.86 ± 85.33	.43
Hb (g/dL)	11.45 ± 2.31	13.57 ± 3.65	<.0001	11.84 ± 6.56	12.62 ± 1.91	<.0001
GGT (U/L)	176.64 ± 223.19	125.07 ± 209.30	.005	288.95 ± 254.94	210.77 ± 248.65	<.0001
Bilirubin (mg/dL)	2.08 ± 3.25	1.05 ± 1.10	<.0001	2.34 ± 3.56	1.29 ± 1.99	<.0001
PT	15.85 ± 2.07	14.44 ± 1.51	<.0001	15.25 ± 2.35	14.51 ± 1.69	<.0001
Albumin (g/dL)	3.01 ± 0.32	4.0 ± 0.37	<.0001	2.92 ± 0.30	3.90 ± 0.33	<.0001
AST (U/L)	79.91 ± 88.61	68.38 ± 122.83	<.0001	146.69 ± 304.91	83.36 ± 97.02	<.0001
AFP (ULN[b])	23.47 ± 16.58	8.29 ± 17.05	<.0001	46.98 ± 17.52	21.73 ± 19.43	<.0001
MTD (cm)	2.84 ± 1.17	2.75 ± 1.19	.478	10.44 ± 3.48	8.65 ± 3.09	<.0001
PVT (%)	33(28.7)	10(8.3)	<.0001[c]	210(77.2)	56(45.2)	<.0001[c]
Nodules>3, n (%)	61 (53)	32 (26.7)	<.0001[c]	163(59.9)	45 (36.3)	<.0001[c]

Values are means ± stand deviation.

Abbreviations: AFP, α-fetoprotein; AST, aspartate aminotransaminase; GGT, γ-glutamyl transpeptidase; Hb, hemoglobin; HCC, hepatocellular carcinoma; MTD, maximum tumor diameter; PT, prothrombin time; PVT, portal vein thrombosis.

[a]Wilcoxon rank sum (Mann-Whitney) test.

[b]Divided by the upper limit of the normal range.

[c]Chi-squared test.

TABLE 2 Comparisons between patients with HCC with serum albumin dichotomized into <3.5 or ≥3.5 g/dL, and bilirubin <2.0 mg/dL

	Small tumours (<5 cm diameter)			Large tumours (≥5 cm diameter)		
	Albumin <3.5	Albumin ≥3.5		Albumin <3.5	Albumin ≥3.5	
Parameter	(n = 87)	(n = 112)	*P* value[a]	(n = 201)	(n = 115)	*P* value[a]
AFP (ULN[b])	22.40 ± 15.78	16.97 ± 92.26	<.0001	34.68 ± 41.36	21.31 ± 19.55	<.0001
MTD (cm)	2.79 ± 1.18	2.78 ± 1.20	.883	10.57 ± 3.48	8.62 ± 3.02	<.0001
PVT (%)	24(27.6%)	10(9.1%)	.001[c]	151(75.1%)	52(45.2%)	<.0001[c]
Nodules>3,n(%)	45(51.7%)	30(26.8%)	<.0001[c]	124(61.7%)	43(37.4%)	<.0001[c]

Values are means ± standard deviation.

Abbreviations: AFP, α-fetoprotein; HCC, hepatocellular carcinoma; MTD, maximum tumour diameter; PVT, portal vein thrombosis.

[a]Wilcoxon rank sum (Mann–Whitney) test.

[b]divided by the upper limit of the normal range.

[c]Chi-squared test.

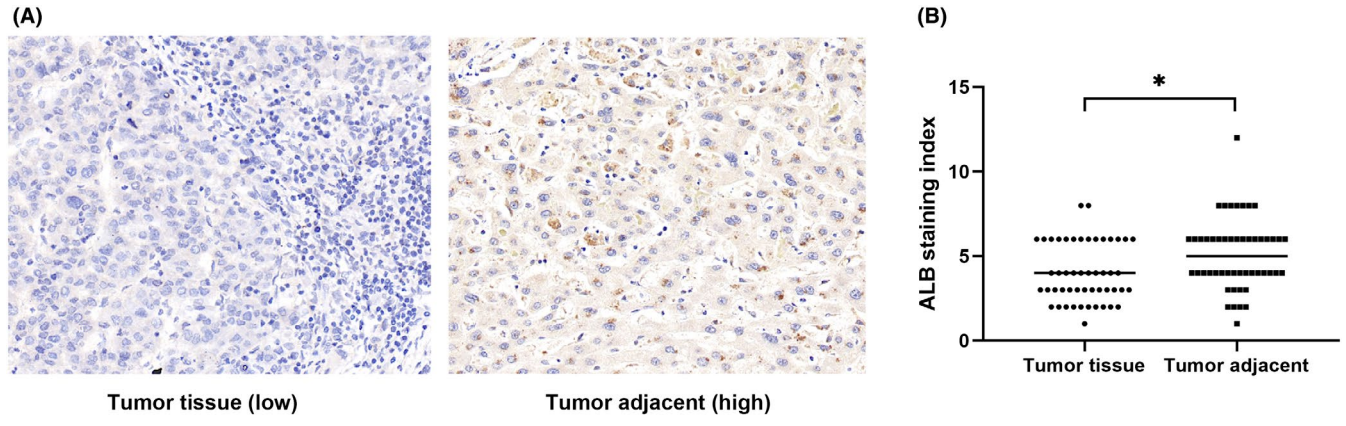

FIGURE 1 A, Representative immunohistochemistry staining of ALB in hepatocellular carcinoma (HCC) tissue and tumour-adjacent tissues. B, ALB staining index are significantly lower in HCC tissue compared with matched HCC tumour-adjacent tissues

ALB levels and clinical-pathological features of HCC was analysed and ALB expression was significantly correlated with vascular invasion ($P = .011$), differentiation ($P = .033$), and TNM stage ($P = .02$) (Table 3). The results demonstrated that ALB might correlate with HCC metastasis.

3.3 | Expression of ALB in L02, Huh7, Hep3B, HepG2 and MHCC97H cells

We conducted western blot analysis with liver cancer cell lines Huh7, Hep3B, HepG2 and MHCC97H which have different metastatic potential than normal liver cell L02 line (Figure 2A). The results showed remarkably downregulated ALB in the four HCC cell lines compared with L02 ($P < .05$) (Figure 2B). The level of ALB in the highly metastatic MHCC-97H cell line was reduced compared with the HCC cell lines with lower metastatic potential (Huh-7, HepG2) (Figure 2B), indicating that the metastatic ability of HCC was related to the downregulation of ALB. Therefore, Huh-7 and HepG2 cell lines were considered for subsequent experiments.

TABLE 3 Correlation between ALB expression and clinicopathological parameters of hepatocellular carcinoma

Variables	All patients (n = 50)	ALB expression		*P* value
		Low	High	
Age (years)				
≤55	28	16	12	.642
>55	22	14	8	
Gender				
Male	44	14	30	.941
Female	6	2	4	
Tumour size (cm)				
≤5	29	13	16	.39
>5	21	12	9	
Tumour number				
Single	30	18	12	.166
Multiple	20	8	12	
Vascular invasion				
Yes	12	4	8	.011*
No	38	28	10	
Differentiation				
Well + moderate	37	24	13	.033*
Poor	13	4	9	
TNM stage				
I-II	32	14	18	.02*
III-IV	18	14	4	

High means IHC score≥6 Low means IHC score < 6. *$P < 0.05$ was considered statistically significant.

3.4 | Effects of ALB knockdown on HepG2 and Huh-7 migration and invasion

Wound healing and Transwell assays were conducted to evaluate the effects of ALB knockdown on the migration and invasion abilities of Huh-7 and HepG2 cells. Western blot analysis showed that ALB specific-siRNA suppressed both intracellular and extracellular expression of ALB (Figure 2C,F). The results of the migration and invasion assays showed that ALB knockdown group significantly promoted the migration of HepG2 and Huh-7 cells, compared against the negative control group (Figure 3A,B). The Transwell assay results showed a significantly higher ability of HepG2 and Huh-7 cells to invade, as compared to the control cell group (Figure 3C,D,E).

3.5 | iTRAQ quantification of the ALB interactome and go analysis

A flow chart is displayed in FigureS1 illustrating the iTRAQ marking and detection process. Prior to iTRAQ-based MS detection, the knockdown efficiency of ALB was measured, and the results showed that ALB expression was inhibited compared against the control group (Figure 2F). An additional ±2.0-fold cut-off was used to evaluate iTRAQ ratios to define the DEPs precisely.[19,20] A total of 210 secretory DEPs were identified, 30 of which were upregulated and 180 that were downregulated (Table S1). Table 4 presents the top 10 up-regulated and down-regulated proteins. The cellular components, biological processes, and molecular functions of the DEPs were identified via PANTHER. The DEPs held 27 biological processes, 18 cellular components and 10 molecular functions (Figure S2). Cellular, metabolic processes, and biological regulation were the most common biological processes, while binding and catalytic activity were the most common molecular functions.

3.6 | KEGG pathway enrichment analysis

KEGG pathway enrichment analysis was performed to identify the functions of DEPs. The results showed that the ALB interactome was classified into 20 pathways (Figure S3). The complement and coagulation cascades pathway was the top pathway. The KEGG map related to the complement and coagulation cascades pathway suggested a potential functional as an essential protein – uPAR, in the molecular mechanism of invasion and metastasis, as shown in Figure 4.

3.7 | Validation of DEPs

According to the iTRAQ outcomes, 10 proteins were selected from 210 DEPs. The mRNA expression of AZGP1 (zinc alpha2 glycoprotein), GPC3 (glypican-3), CTSF (Cathepsin F), NOTCH1

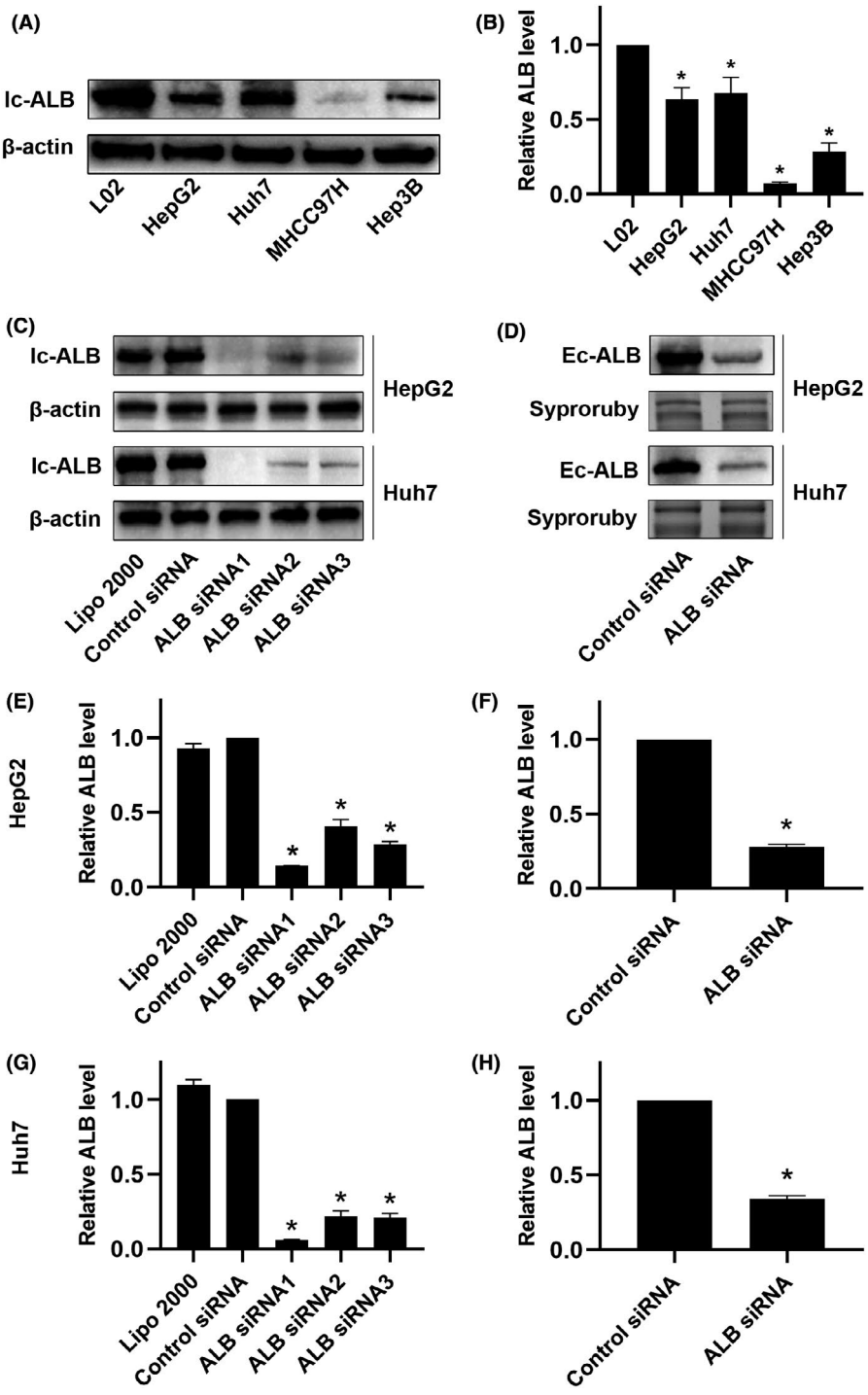

FIGURE 2 A, B, The expression of ALB was lower in hepatocellular carcinoma (HCC) cell lines compared with the normal L02 cells assessed by western blot. C, E, and G, Cells were transfected with ALB-targeted siRNAs. Western blot analysis shows that the silencing of ALB significantly reduced ALB protein levels, intracellular ALB (Ic-ALB) of HepG2 and Huh7 cells. D, F and H, Cells were transfected with ALB-targeted siRNA. Western blot analysis shows that the silencing of ALB significantly reduced ALB protein levels, extracellular ALB (Ec-ALB) of HepG2 and Huh7 cells

(neurogenic locus notch homolog protein 1), CTSD (cathepsin D), uPAR, BMP2 (bone morphogenetic protein 2), LCN2 (lipocalin 2), IDH2 (isocitrate dehydrogenase 2) and RPS3A (ribosomal protein S3a) was detected by RT-qPCR, relative to GAPDH. After knockdown of ALB, the mRNA expression levels of AZGP1, GPC3, CTSF, CTSD, BMP2 and LCN2 were significantly decreased, while NOTCH1, uPAR, IDH2 and RPS3A were increased (Figure 5A). The expression levels of AZGP1, GPC3, NOTCH1, CTSD, uPAR, BMP2, LCN2, IDH2 and RPS3A were validated using western blot analysis (Figure 5B). Both results were consistent with the iTRAQ data. We selected three key DEPs for further evaluation. Wound healing and the Matrigel invasion assay were applied to examine the migrated and invasive potential of RPS3A, NOTCH1 and uPAR silenced cells. Western blot analysis showed that RPS3A, NOTCH1 and uPAR specific-siRNA decreased the expression of RPS3A, NOTCH1 and uPAR (Figure 6A-C). The results of the wound healing showed that uPAR knockdown group significantly inhibited the migration of HepG2 and Huh-7 cells, compared with the negative

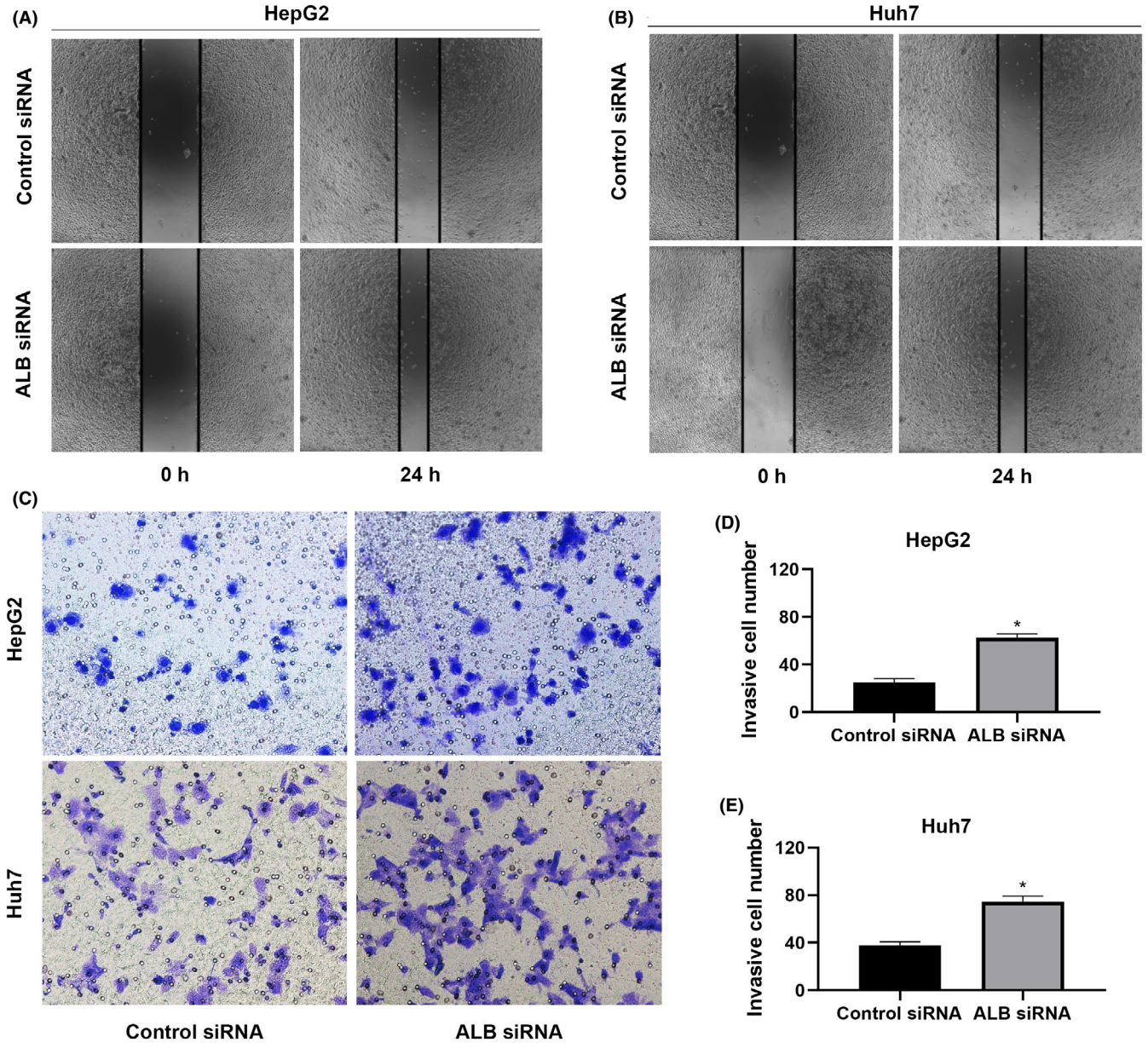

FIGURE 3 A, B, Wound healing assays using ALB-knockdown cells in HepG2 and Huh7; C, D, Representative images and quantification of the effects of ALB silencing on the invasive abilities of HepG2 cells as determined by Transwell assay. C, E, Representative images and quantification of the effects of ALB silencing on the invasive abilities of Huh7 cells as determined by Transwell assay. Data represent the mean ± SD from three independent experiments. $*P < .05$

control group (Figure 6D). As illustrated in Figure 6E and F, uPAR siRNA transfected cells showed a significantly lower level of penetration through the Matrigel-coated membrane compared with the control cell group.

3.8 | ALB knockdown on matrix metalloproteinases and epithelial–mesenchymal transition in liver cancer

On account of the functional involvement of uPAR in cell adhesion, migration and proliferation, and because we found it to be upregulated in the KEGG-enriched pathway (Figure 4), we concluded that there was a link between ALB and uPAR protein. Epithelial–mesenchymal transition (EMT) and matrix metalloproteinases (MMPs) are important markers for tumour metastatic potential and aggressive growth. The uPA/uPAR system has been shown to be related to the MMP-9 activation, the subsequent degradation of the extracellular matrix, and increased invasion.[19] The invasion related genes MMPs and EMT-associated markers, E-cadherin, N-cadherin, vimentin and transcription factors, Snail and Twist, were detected by western blot analysis to analyse the effects of ALB knockdown on HCC migration and invasion. Inhibition of ALB significantly increased the expression and

TABLE 4 The top 10 upregulated and downregulated differentially expressed proteins, as identified using iTRAQ technology

N	Accession no.	Gene symbol	Protein name	ALB Knockdown vs control	*P* value
Top 10 proteins upregulated in ALB siRNA secretory protein					
1	sp|Q96M20|CNBD2_HUMAN	CNBD2	Cyclic nucleotide-binding domain-containing protein 2	4.37	.0088
2	sp|Q8N5V2|NGEF_HUMAN	NGEF	Ephexin-1	4.26	.0158
3	sp|Q5TDP6|LGSN_HUMAN	LGSN	Lengsin	4.02	.0002
4	sp|Q8TET4|GANC_HUMAN	GANC	Neutral alpha-glucosidase C	3.71	.0041
5	sp|Q03405|UPAR_HUMAN	PLAUR	Urokinase plasminogen activator surface receptor	3.52	.0000
6	sp|Q9UH62|ARMX3_HUMAN	ARMCX3	Armadillo repeat-containing X-linked protein 3	3.44	.0014
7	sp|P48735|IDHP_HUMAN	IDH2	Isocitrate dehydrogenase [NADP], mitochondrial	3.38	.0092
8	sp|O00562|PITM1_HUMAN	PITPNM1	Membrane-associated phosphatidylinositol transfer protein 1	3.31	.0039
9	sp|P11166|GTR1_HUMAN	SLC2A1	Solute carrier family 2, facilitated glucose transporter member 1	2.85	.0000
10	sp|Q96A70|AZIN2_HUMAN	AZIN2	Antizyme inhibitor 2	2.77	.0000
Top 10 proteins downregulated in ALB siRNA secretory protein					
1	sp|P02647|APOA1_HUMAN	APOA1	Apolipoprotein A-I	0.18	.0000
2	sp|P20142|PEPC_HUMAN	PGC	Gastricsin	0.18	.0000
3	sp|P80188|NGAL_HUMAN	LCN2	Neutrophil gelatinase-associated lipocalin	0.19	.0000
4	sp|Q9BRK5|CAB45_HUMAN	SDF4	45 kDa calcium-binding protein	0.2	.0000
5	sp|P02749|APOH_HUMAN	APOH	Beta-2-glycoprotein 1	0.21	.0000
6	sp|Q15904|VAS1_HUMAN	ATP6AP1	V-type proton ATPase subunit S1	0.23	.0000
7	sp|P05156|CFAI_HUMAN	CFI	Complement factor I	0.25	.0000
8	sp|P02652|APOA2_HUMAN	APOA2	Apolipoprotein A-II	0.25	.0000
9	sp|P36955|PEDF_HUMAN	SERPINF1	Pigment epithelium-derived factor	0.26	.0000
10	sp|P00739|HPTR_HUMAN	HPR	Haptoglobin-related protein	0.26	.0000

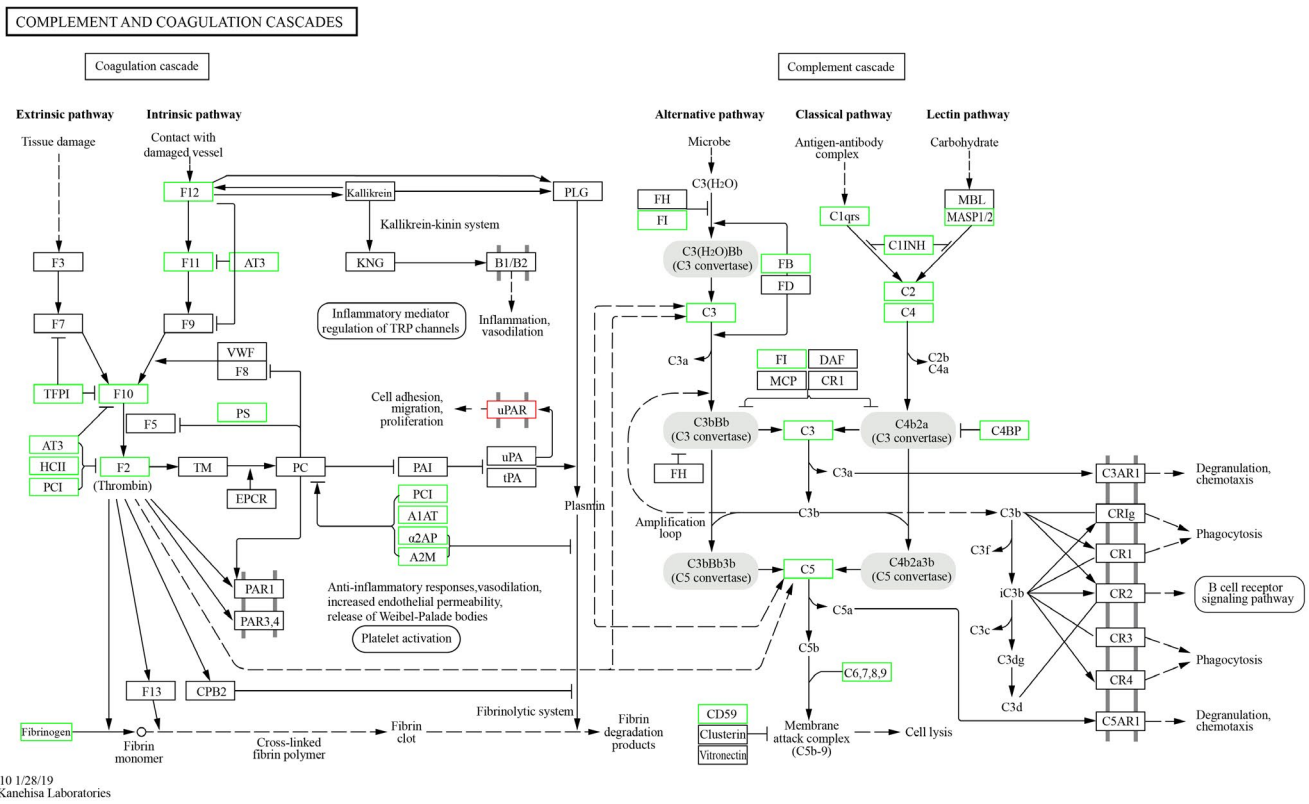

FIGURE 4 Complement and coagulation cascades pathway map. KEGG pathway enrichment analysis the map of the complement and coagulation cascades pathway. Proteins in colourful frames show differentially expressed proteins. The green frames indicate down-regulated proteins, whereas the red frame indicates up-regulated protein

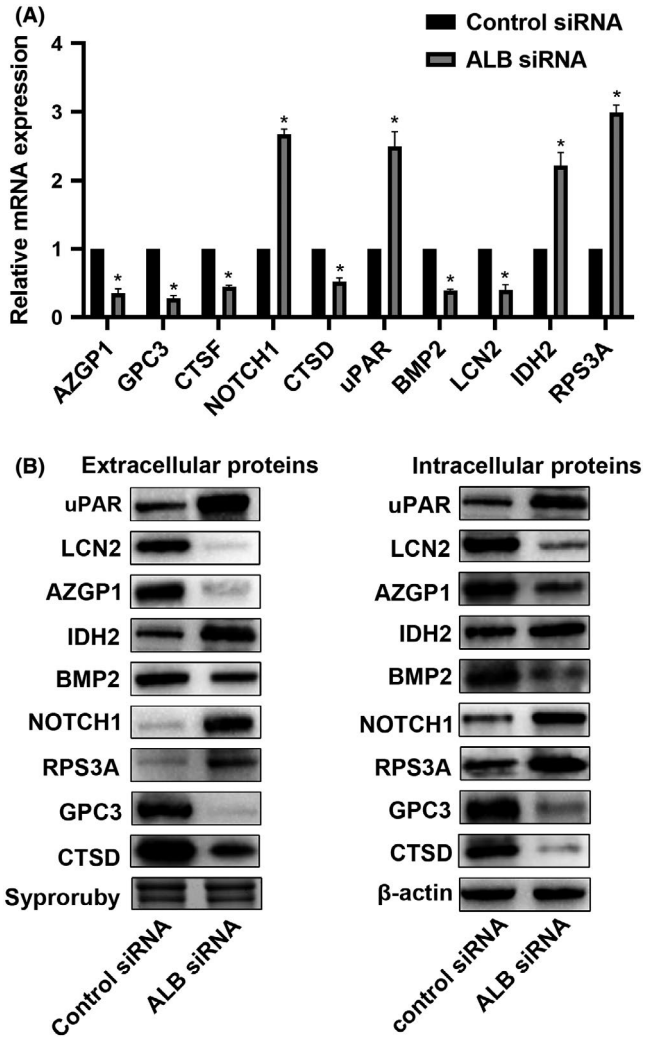

FIGURE 5 Verification of the differentially expressed proteins. A, the RT-PCR detected the relative mRNA expression levels of AZGP1, GPC3, CTSF, NOTCH1, CTSD, uPAR, BMP2, LCN2, IDH2 and RPS3A (*$P < .05$). B, A representative western blot analysis for AZGP1, GPC3, NOTCH1, CTSD, uPAR, BMP2, LCN2, IDH2 and RPS3A expression in intracellular and extracellular samples from HepG2 cells. (Bars indicate SD, *$P < .05$)

activity of MMP2 and MMP9 in HepG2 and Huh7 cells (Figure 7A). Zymography revealed strong MMP-2 and MMP9 activity in HepG2 and Huh7, respectively (Figure 7B). As demonstrated in Figure 7C, knockdown of ALB significantly increased the expression of N-cadherin, vimentin, Snail and Twist, and decreased E-cadherin in HepG2 and Huh7 cells.

3.9 | Validation of the interaction between ALB and uPAR

The key protein-uPAR was confirmed using ELISA in a validation cohort. The serum level of uPAR was measured in 108 cases, including 36 HCC (ALB ≥3.5 g/dL), 34 HCC (ALB <3.5 g/dL), 19 CH and 19 LC. The concentration of uPAR was significantly higher in the HCC subgroup (ALB <3.5 g/dL) than that in the ALB ≥ 3.5 g/dL group ($P < .05$) (Figure 7D), but no significant difference was observed between the CHB and LC groups (data not shown). Furthermore, to determine a correlation between ALB and uPAR in HCC, Spearman's correlation analysis demonstrated a negative correlation between ALB and uPAR expression in the HCC group (Figure 7E).

4 | DISCUSSION

ALB plays a role in several human disorders and diseases, such as inflammation, diabetes, cardiovascular diseases, chronic nephropathies, and cancer.[20-24] ALB has been shown to have a direct growth-suppression property in various malignant tumours, such as breast and HCC cancers.[25,26] Additionally, there is clinical manifestation of suppressive effect on patients with HCC.[27,28] However, few studies have reported its effects on invasion and migration abilities in HCC cells.

In the clinical HCC cohort study, we observed that albumin levels were negatively correlated with tumour aggression parameters, including MTD, PVT and AFP, especially in tumours with diameters >5 cm. Higher levels of bilirubin may be a clinical cofounding factor which cannot reflect the actual liver function. However, during subgroup analysis including only patients having normal bilirubin levels, a similar correlation was found.

Here, we measured the expression of ALB and found low expression in HCC tissues and cells. Combined with clinical characteristics, our results showed a significant correlation between the absence of vascular invasion, higher TNM staging, and more inadequate differentiation of HCC ($P < .05$). Western blot revealed that ALB levels in the highly-metastatic HCC cell line MHCC-97H were considerably lower than in the less-metastatic HepG2 and Huh-7 cell lines, indicating that downregulation of ALB was linked to the metastatic ability of HCC. We further demonstrated that ALB knockdown in HepG2 and Huh7 cells increased migration and invasion in the wound and Transwell assays. This is the first report of ALB inhibiting tumour cell migration and invasion, suggesting that ALB is a potential antioncogene.

To illustrate the molecular mechanism of ALB in migration and invasion of HCC, we identified secreted DEPs in ALB knockdown and negative HepG2 cells by using iTRAQ and MS. Based on the GO analysis, the interacting DEPs were focused on cellular, metabolic processes and biological regulation. According to a KEGG pathway enrichment analysis, the complement and coagulation cascades pathway was the most significantly enriched. Most identified proteins interacting with ALB were enriched for this pathway. The KEGG map related to the complement and coagulation cascades pathway suggested a functionally vital role in the mechanism of invasion and metastasis. A number of essential proteins, including AZGP1, GPC3, CTSF, NOTCH1, CTSD, uPAR, BMP2, LCN2, IDH2 and RPS3A, were identified using RT-PCR and western blot analyses.

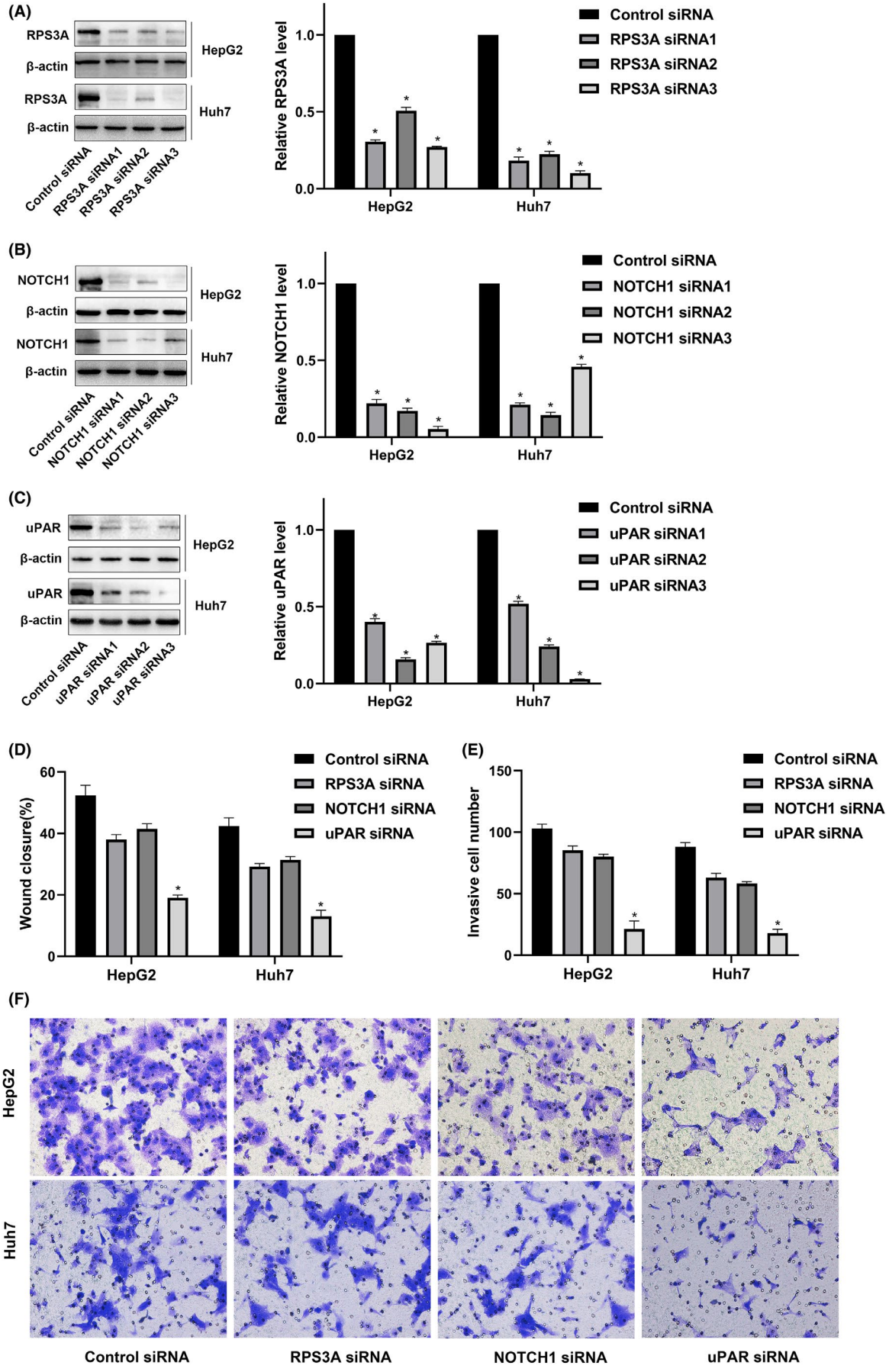
(A)
RPS3A
β-actin
RPS3A
β-actin
HepG2
Huh7
Control siRNA
RPS3A siRNA1
RPS3A siRNA2
RPS3A siRNA3
Relative RPS3A level
1.0
0.5
0.0
HepG2
Huh7
Control siRNA
RPS3A siRNA1
RPS3A siRNA2
RPS3A siRNA3
(B)
NOTCH1
β-actin
NOTCH1
β-actin
HepG2
Huh7
Control siRNA
NOTCH1 siRNA1
NOTCH1 siRNA2
NOTCH1 siRNA3
Relative NOTCH1 level
1.0
0.5
0.0
HepG2
Huh7
Control siRNA
NOTCH1 siRNA1
NOTCH1 siRNA2
NOTCH1 siRNA3
(C)
uPAR
β-actin
uPAR
β-actin
HepG2
Huh7
Control siRNA
uPAR siRNA1
uPAR siRNA2
uPAR siRNA3
Relative uPAR level
1.0
0.5
0.0
HepG2
Huh7
Control siRNA
uPAR siRNA1
uPAR siRNA2
uPAR siRNA3
(D)
Wound closure(%)
60
40
20
0
HepG2
Huh7
Control siRNA
RPS3A siRNA
NOTCH1 siRNA
uPAR siRNA
(E)
Invasive cell number
150
100
50
0
HepG2
Huh7
Control siRNA
RPS3A siRNA
NOTCH1 siRNA
uPAR siRNA
(F)
HepG2
Huh7
Control siRNA
RPS3A siRNA
NOTCH1 siRNA
uPAR siRNA

FIGURE 6 A-C, Cells were transfected with RPS3A, NOTCH1, uPAR-targeted siRNAs. Western blot analysis shows that the silencing of RPS3A, NOTCH1, uPAR significantly reduced RPS3A, NOTCH1, uPAR protein levels. D, Analysis of wound closure (%) using RPS3A, NOTCH1, uPAR-knockdown cells in HepG2 and Huh7. E, F, Representative images and quantification of the effects of RPS3A, NOTCH1, uPAR silencing on the invasive abilities of HepG2 and Huh7 cells as determined by Transwell assay. Data represent the mean ± SD from three independent experiments. $*P < .05$

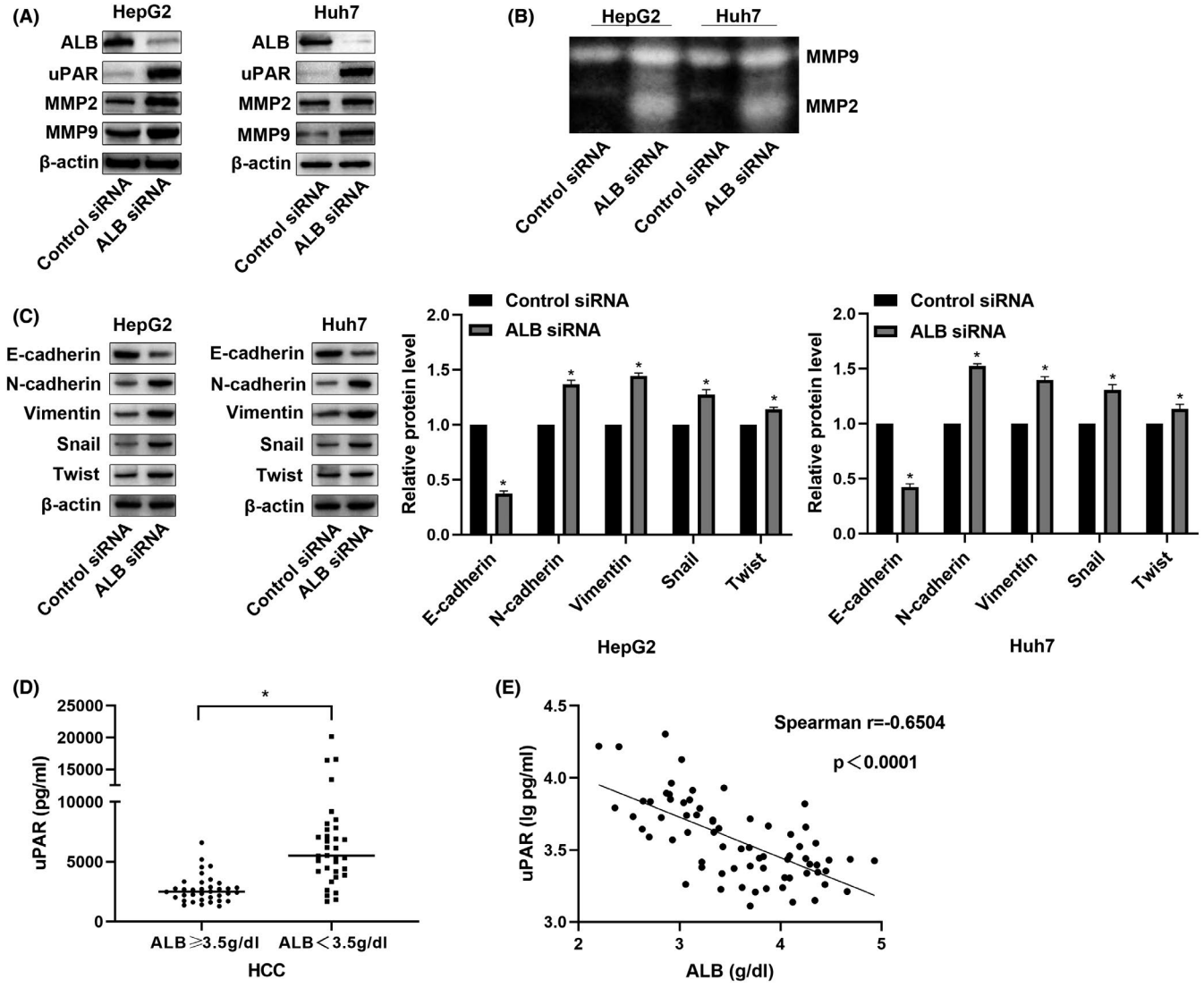

FIGURE 7 A, Representative images of the western blot results for uPAR, MMP2 and MMP9 in ALB knockdown HepG2 and Huh7 cells; B, Zymography analysis illustrates MMP2 and MMP9 activity in ALB knockdown HepG2 and Huh7 cells; C, Quantitative analysis results and representative images of the western blot results for the EMT-associated markers, E-cadherin, N-cadherin, vimentin, Snail and Twist by western blot in ALB knockdown HepG2 and Huh7 cells; D, Quantification shows a significantly higher uPAR in HCC group with ALB <3.5 g/dL compared to ALB ≥3.5 g/dL ($*P < .05$); E, Scatterplot showing the correlation between plasma levels of ALB and uPAR. The vertical position represents the expression levels of uPAR (lg pg/mL)

To investigate the mechanisms by which ALB could regulate HCC progression, we selected several proteins (RPS3A, NOTCH1 and uPAR) for further evaluation. RPS3A, a component of the 40S ribosome small subunit, plays a vital role in cell transformation, growth and several types of tumour such as HCC,[29,30] thyroid carcinoma,[31] colorectal cancer[32] and lung cancer.[33] Previous study reported that RPS3A regulate NF-κB activity to promote the progress of HBV-induced HCC.[34] It can promote carcinogenesis of HCC by activating he ERK and mTOR pathways. High RPS3A expression is associated with low tumour immune cell infiltration and poor prognosis in patients with HCC.[35]

NOTCH family was first identified in drosophila melanogaster, regulate embryonic development and transfer signals.[36] Previous studies suggested that NOTCH1 is involved in tumorigenesis, and

associated with cell proliferation, apoptosis, migration and invasion.[37-39] NOTCH1 plays a key role in the invasion and metastasis of cancer via various signalling molecules and pathways. For example, Zhou et al and Li et al demonstrated that NOTCH1 regulate Snail/E-cadherin through cyclooxygenase-2 (COX-2) or PTEN-FAK pathway.[40,41] NOTCH1 affects HCC progression through regulating EMT and vasculogenic mimicry formation.[42] NOTCH1 promotes hepatitis B virus X protein-induced hepatocarcinogenesis through Wnt/β-catenin signalling.[43] Knockdown of RPS3A, NOTCH1 and uPAR in HepG2 and Huh7 cells by siRNA, the results indicated that the down-regulation of uPAR significantly inhibits the migration and invasion of HCC cells.

Taking together, we focused on the critical protein uPAR, which plays a vital role in cell adhesion, migration, and proliferation. The levels of uPAR, also named PLAUR, were increased in ALB-knockdown HepG2 cell lines. uPAR has been reported to play a significant role in inflammation, immune suppression, cancer progression and metastasis,[44,45] and thus it indicates poor prognosis, especially in HCC. uPAR is elevated in many human cancers, including oral squamous cell, breast, cervical, bladder and HCCs.[46-50] EMT has a key role in cancer progression and is associated with migration and invasion.[51,52] MMPs are secreted from both tumour and stroma cells and contribute to tumour metastasis regulation by degrading the extracellular matrix.[53,54] Previous studies have reported that uPAR, MMP-2 and MMP-9, as crucial components of the extracellular matrix degradation process, are associated with the cell events such as growth, migration, invasion and survival in many types of cancer.[53] In addition, we confirmed that knockdown of uPAR could significantly rescue the metastatic behaviours of ALB knockdown in HCC cells. Therefore, those data confirmed that ALB could suppress HCC metastasis via regulating the uPAR signalling. Interestingly, our results indicated that silencing ALB expression in HCC cells elevates the expression of EMT-related biomarkers, including MMP2, MMP9 and uPAR. Subsequent clinical validation cohort analysis revealed that there was a negative correlation between ALB and uPAR expression in the HCC patient group, suggesting a new mechanism for ALB interacting with uPAR to suppress the invasion and metastasis of HCC induced by MMPs.

5 | CONCLUSION

This is the first report that ALB functions as a tumour suppressor. Knockdown of ALB promotes HCC progression. Based on the 210 secretory DEPs selected from the iTRAQ-based proteomics analysis, the critical protein-uPAR that interacts with ALB is associated with tumour biological behaviours. Down-regulation of ALB promotes HCC migration and invasion by increasing expression of uPAR and MMPs. However, further investigation is necessary to determine the precise mechanism of ALB in the progression of HCC.

CONFLICT OF INTEREST

None.

DATA AVAILABILITY STATEMENT

The data that support the findings of this study are available from the corresponding author upon reasonable request.

ORCID

Dazhi Zhang https://orcid.org/0000-0001-5382-9822

REFERENCES

1. Bray F, Ferlay J, Soerjomataram I, Siegel RL, Torre LA, Jemal A. Global cancer statistics 2018: GLOBOCAN estimates of incidence and mortality worldwide for 36 cancers in 185 countries. *CA Cancer J Clin*. 2018;68:394–424.
2. Clark T, Maximin S, Meier J, Pokharel S, Bhargava P. Hepatocellular carcinoma: review of epidemiology, screening, imaging diagnosis, response assessment, and treatment. *Curr Probl Diagn Radiol*. 2015;44:479–486.
3. Siegel RL, Miller KD, Jemal A. Cancer statistics, 2019. *CA Cancer J Clin*. 2019;69:7–34.
4. Colecchia A, Schiumerini R, Cucchetti A, et al. Prognostic factors for hepatocellular carcinoma recurrence. *World J Gastroenterol*. 2014;20:5935–5950.
5. Rodriguez-Peralvarez M, Luong TV, Andreana L, Meyer T, Dhillon AP, Burroughs AK. A systematic review of microvascular invasion in hepatocellular carcinoma: diagnostic and prognostic variability. *Ann Surg Oncol*. 2013;20:325–339.
6. Wang D, Hu XI, Xiao L, et al. Prognostic nutritional index and systemic immune-inflammation index predict the prognosis of patients with HCC. *J Gastrointest Surg*. 2021;25:421–427.
7. Pang S, Zhou Z, Yu X, et al. The predictive value of integrated inflammation scores in the survival of patients with resected hepatocellular carcinoma: a retrospective cohort study. *Int J Surg*. 2017;42:170–177.
8. Yamamoto M, Kobayashi T, Kuroda S, et al. Verification of inflammation-based prognostic marker as a prognostic indicator in hepatocellular carcinoma. *Ann Gastroenterol Surg*. 2019;3:667–675.
9. Quinlan GJ, Martin GS, Evans TW. Albumin: biochemical properties and therapeutic potential. *Hepatology*. 2005;41:1211–1219.
10. Carr BI, Guerra V. Validation of a liver index and its significance for HCC aggressiveness. *J Gastrointest Cancer*. 2017;48:262–266.
11. Nojiri S, Joh T. Albumin suppresses human hepatocellular carcinoma proliferation and the cell cycle. *Int J Mol Sci*. 2014;15:5163–5174.
12. Carr BI, Guerra V. Serum albumin levels in relation to tumor parameters in hepatocellular carcinoma patients. *Int J Biol Markers*. 2017;32:e391–e396.
13. Iadarola P. Special issue: mass spectrometric proteomics. *Molecules*. 2019;24:6.
14. O'Neill JR. An overview of mass spectrometry-based methods for functional proteomics. *Methods Mol Biol*. 2019;1871:179–196.
15. Marrero JA, Kulik LM, Sirlin CB, et al. Diagnosis, staging, and management of hepatocellular carcinoma: 2018 practice guidance by the American Association for the Study of Liver Diseases. *Hepatology*. 2018;68:723–750.
16. Huang J, Tang Y, Zou X, et al. Identification of the fatty acid synthase interaction network via iTRAQ-based proteomics indicates the potential molecular mechanisms of liver cancer metastasis. *Cancer Cell Int*. 2020;20:332.
17. Wang K, Wang X, Zheng S, et al. iTRAQ-based quantitative analysis of age-specific variations in salivary proteome of caries-susceptible individuals. *J Transl Med*. 2018;16:293.
18. Schmittgen TD, Livak KJ. Analyzing real-time PCR data by the comparative C(T) method. *Nat Protoc*. 2008;3:1101–1108.

19. Dass K, Ahmad A, Azmi AS, Sarkar SH, Sarkar FH. Evolving role of uPA/uPAR system in human cancers. *Cancer Treat Rev*. 2008;34:122–136.
20. Lv L-L, Feng YE, Wen YI, et al. Exosomal CCL2 from tubular epithelial cells is critical for albumin-induced tubulointerstitial inflammation. *J Am Soc Nephrol*. 2018;29:919–935.
21. Arques S. Human serum albumin in cardiovascular diseases. *Eur J Intern Med*. 2018;52:8–12.
22. Gupta D, Lis CG. Pretreatment serum albumin as a predictor of cancer survival: a systematic review of the epidemiological literature. *Nutr J*. 2010;9(1):69.
23. Eckart A, Struja T, Kutz A, et al. Relationship of nutritional status, inflammation, and serum albumin levels during acute illness: a prospective study. *Am J Med*. 2020;133:713–722 e717.
24. Peavy DE, Taylor JM, Jefferson LS. Time course of changes in albumin synthesis and mRNA in diabetic and insulin-treated diabetic rats. *Am J Physiol*. 1985;248(6 Pt 1):E656–663.
25. Laursen I, Briand P, Lykkesfeldt AE. Serum albumin as a modulator on growth of the human breast cancer cell line, MCF-7. *Anticancer Res*. 1990;10:343–351.
26. Bağırsakçı E, Şahin E, Atabey N, Erdal E, Guerra V, Carr BI. Role of albumin in growth inhibition in hepatocellular carcinoma. *Oncology*. 2017;93:136–142.
27. Nagao Y, Sata M. Serum albumin and mortality risk in a hyperendemic area of HCV infection in Japan. *Virol J*. 2010;7:375.
28. Wong V-S, Chan SL, Mo F, et al. Clinical scoring system to predict hepatocellular carcinoma in chronic hepatitis B carriers. *J Clin Oncol*. 2010;28:1660–1665.
29. Kim M-Y, Park E, Park J-H, et al. Expression profile of nine novel genes differentially expressed in hepatitis B virus-associated hepatocellular carcinomas. *Oncogene*. 2001;20:4568–4575.
30. Shuda M, Kondoh N, Tanaka K, et al. Enhanced expression of translation factor mRNAs in hepatocellular carcinoma. *Anticancer Res*. 2000;20:2489–2494.
31. Musholt TJ, Goodfellow PJ, Scheumann GF, Pichlmayr R, Wells SA Jr, Moley JF. Differential display in primary and metastatic medullary thyroid carcinoma. *J Surg Res*. 1997;69:94–100.
32. Pogue-Geile K, Geiser JR, Shu M, et al. Ribosomal protein genes are overexpressed in colorectal cancer: isolation of a cDNA clone encoding the human S3 ribosomal protein. *Mol Cell Biol*. 1991;11:3842–3849.
33. Slizhikova DK, Vinogradova TV, Sverdlov ED. The NOLA2 and RPS3A genes as highly informative markers for human squamous cell lung cancer. *Bioorg Khim*. 2005;31:195–199.
34. Lim K-H, Kim K-H, Choi SI, et al. RPS3a over-expressed in HBV-associated hepatocellular carcinoma enhances the HBx-induced NF-κB signaling via its novel chaperoning function. *PLoS One*. 2011;6:e22258.
35. Zhou C, Weng J, Liu C, et al. High RPS3A expression correlates with low tumor immune cell infiltration and unfavorable prognosis in hepatocellular carcinoma patients. *Am J Cancer Res*. 2020;10:2768–2784.
36. Yamamoto S. Making sense out of missense mutations: Mechanistic dissection of Notch receptors through structure-function studies in Drosophila. *Dev Growth Differ*. 2020;62:15–34.
37. Jackstadt R, van Hooff SR, Leach JD, et al. Epithelial NOTCH signaling rewires the tumor microenvironment of colorectal cancer to drive poor-prognosis subtypes and metastasis. *Cancer Cell*. 2019;36:319–336.e317.
38. Hu J, Yu J, Gan J, et al. Notch1/2/3/4 are prognostic biomarker and correlated with immune infiltrates in gastric cancer. *Aging (Albany NY)*. 2020;12:2595–2609.
39. Gan R-H, Wei H, Xie J, et al. Notch1 regulates tongue cancer cells proliferation, apoptosis and invasion. *Cell Cycle*. 2018;17:216–224.
40. Zhou L, Wang DS, Li QJ, Sun W, Zhang Y, Dou KF. The down-regulation of Notch1 inhibits the invasion and migration of hepatocellular carcinoma cells by inactivating the cyclooxygenase-2/Snail/E-cadherin pathway in vitro. *Dig Dis Sci*. 2013;58:1016–1025.
41. Li JY, Huang WX, Zhou X, Chen J, Li Z. Numb inhibits epithelial-mesenchymal transition via RBP-Jκ-dependent Notch1/PTEN/FAK signaling pathway in tongue cancer. *BMC Cancer*. 2019;19:391.
42. Jue C, Lin C, Zhisheng Z, et al. Notch1 promotes vasculogenic mimicry in hepatocellular carcinoma by inducing EMT signaling. *Oncotarget*. 2017;8:2501–2513.
43. Sun Q, Wang R, Luo J, et al. Notch1 promotes hepatitis B virus X protein-induced hepatocarcinogenesis via Wnt/β-catenin pathway. *Int J Oncol*. 2014;45:1638–1648.
44. Margheri F, Luciani C, Taddei ML, et al. The receptor for urokinase-plasminogen activator (uPAR) controls plasticity of cancer cell movement in mesenchymal and amoeboid migration style. *Oncotarget*. 2014;5:1538–1553.
45. Yang Q-X, Zhong S, He L, et al. PBK overexpression promotes metastasis of hepatocellular carcinoma via activating ETV4-uPAR signaling pathway. *Cancer Lett*. 2019;452:90–102.
46. Jing J, Zheng S, Han C, Du L, Guo Y, Wang P. Evaluating the value of uPAR of serum and tissue on patients with cervical cancer. *J Clin Lab Anal*. 2012;26:16–21.
47. Hao W, Friedman A. Serum uPAR as biomarker in breast cancer recurrence: a mathematical model. *PLoS One*. 2016;11(4):e0153508.
48. Pavón MA, Arroyo-Solera I, Céspedes MV, Casanova I, León X, Mangues R. uPA/uPAR and SERPINE1 in head and neck cancer: role in tumor resistance, metastasis, prognosis and therapy. *Oncotarget*. 2016;7:57351–57366.
49. Boonstra MC, Van Driel P, Keereweer S, et al. Preclinical uPAR-targeted multimodal imaging of locoregional oral cancer. *Oral Oncol*. 2017;66:1–8.
50. Hau AM, Leivo MZ, Gilder AS, Hu JJ, Gonias SL, Hansel DE. mTORC2 activation is regulated by the urokinase receptor (uPAR) in bladder cancer. *Cell Signal*. 2017;29:96–106.
51. Meng F-D. FoxM1 overexpression promotes epithelial-mesenchymal transition and metastasis of hepatocellular carcinoma. *World J Gastroenterol*. 2015;21:196.
52. Aiello NM, Brabletz T, Kang Y, Nieto MA, Weinberg RA, Stanger BZ. Upholding a role for EMT in pancreatic cancer metastasis. *Nature*. 2017;547:E7–E8.
53. Shi H, Liu L, Liu LM, Geng J, Chen L. Inhibition of tumor growth by beta-elemene through downregulation of the expression of uPA, uPAR, MMP-2, and MMP-9 in a murine intraocular melanoma model. *Melanoma Res*. 2015;25:15–21.
54. Scheau C, Badarau IA, Costache R, et al. The role of matrix metalloproteinases in the epithelial-mesenchymal transition of hepatocellular carcinoma. *Anal Cell Pathol (Amst)*. 2019;2019:9423907.

SUPPORTING INFORMATION

Additional supporting information may be found in the online version of the article at the publisher's website.

How to cite this article: Fu X, Yang Y, Zhang D. Molecular mechanism of albumin in suppressing invasion and metastasis of hepatocellular carcinoma. *Liver Int*. 2022;42:696–709. doi:10.1111/liv.15115